Modifying Stainless Steel Surfaces by Electropolishing

Arian Nadjimzadah

Brighton High School

LLE Advisor: Dr. Walter Shmayda

Abstract

Tritium ingress into stainless steel depends on the surface characteristics of the metal. Electropolishing provides a flexible and controllable method of modifying a metal surface by reducing the surface roughness. A program has been implemented to study the dependence of surface roughness on electrolytic current density, voltage, electrolyte composition, polishing time and operating conditions such as temperature and stir rate. Multiple plots of current density versus potential have been generated at different temperatures as a first step in establishing the appropriate operating electrolytic conditions for a given operating situation. A variety of operating conditions have been tested to obtain a smoother surface and to mitigate surface thickness loss. The precise formation of a viscous layer and the control of gas evolution on the surface have been paramount in developing a macroscopically and microscopically smoother finish.

1. Introduction

Substantial work at LLE has been done to study tritium ingress into stainless steel. Specifically, the tritium and stainless steel interactions studied by Shmayda et al. [1] at LLE are dependent on the surface characteristics of the stainless steel sample. Because of this, stainless steel samples have been sent out to a third party to be electropolished. Unfortunately, the quality of these electropolished samples is somewhat questionable. In this work, the mechanism and operating conditions of electropolishing were studied and progress was made toward optimization.

2. Theory

2.1. Electropolishing on Microscale

Electropolishing works on the basis of an electrolytic cell, as shown in Fig. 1, which summarizes the fundamental chemical processes involved in electropolishing. This consists of a source of electrical potential connected to two electrodes. The electrode located at the deficit region of electrons is known as the anode, and the electrode at the excess region of electrons is known as the cathode. An electrolyte solution is present between the anode and the cathode. This solution is necessary to transfer charge through the solution between the anode and the cathode, which is achieved through the movement of ions in solution. The fundamental principle that drives the cell is the oxidation-reduction reaction. At the anode, oxidation occurs, which results in the dissolution of metals into their constituent ions. Water is also oxidized, evolving oxygen. At the

cathode, reduction occurs, which results in the deposition of metal ions. Water is reduced, which evolves hydrogen. The overall result is a net reduction in anodic mass proportional to the charge applied, which can be quantified by Faraday's Law of Electrolysis:

$$m = \left(\frac{Q}{F}\right)\left(\frac{M}{z}\right) \qquad (1)$$

where m is the mass lost, Q is the total electric charge passed through the anode, F is Faraday's constant, M is the molar mass of the anode, and z is the valency of ions of the substance (the number of electrons transferred per ion).
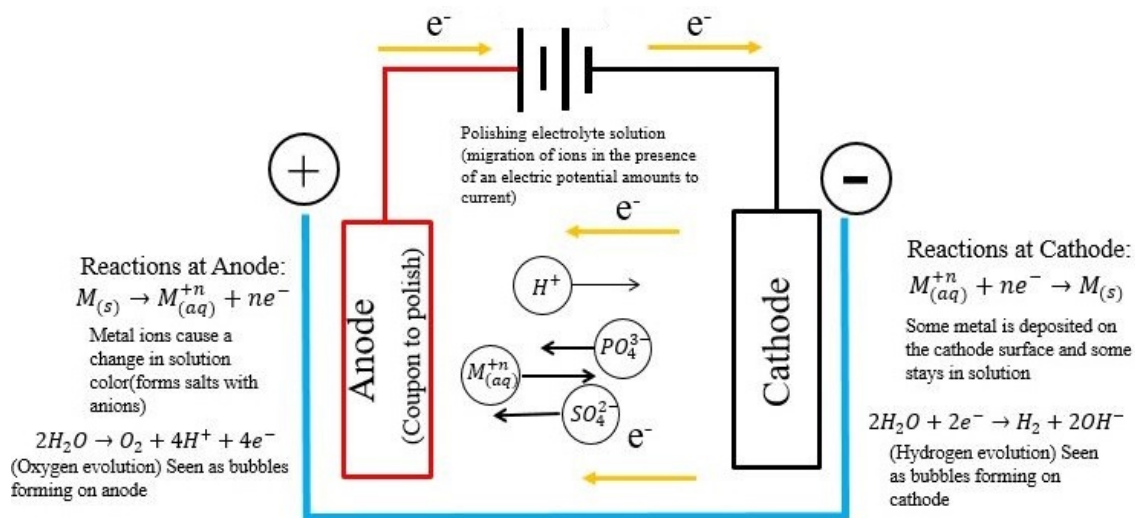

Figure 1: Electrochemical process on microscale. Illustration includes a sulphuric and phosphoric acid electrolyte. Note that a variety of other electrolytes can be used.

2.2. The Viscous Layer and Mass Transfer Mechanism

The chemical reactions detailed above on a large scale are responsible for the mechanism of electropolishing. As metal ions dissolve from the anode surface due to the potential difference, they form a viscous layer which limits the current where the surface concentration is greater than that of the bulk solution. Fig. 2 shows a simplified model of the viscous layer and mass transfer mechanism. According to some theories, the surface metal ion concentration is equal to the saturation concentration, decreasing as the distance from the anode increases [2]. The thickness of this more concentrated metal ion layer is greater in the valleys of the anode than over the peaks.

This results in a lower dissolution in the depressions, because the layer above the surface is already at maximum ion concentration, keeping more dissolution from occurring. Additionally, the thicker viscous layer over the valleys results in an increased resistance, decreasing the current by Ohm's Law. As a consequence of Gauss's Law, electric fields tend to concentrate around peaks, so the current density and dissolution around these regions will increase. All of these factors result in a net leveling of the surface, and a visibly "polished" surface.
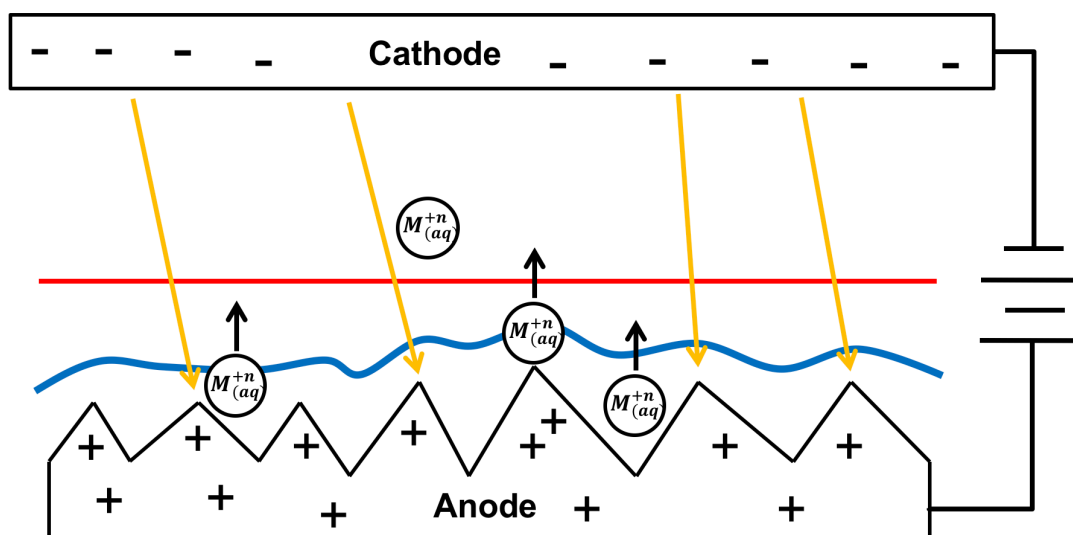

Figure 2: Electrochemical process on macroscale. The viscous layer is represented by the region between the blue curve and the anode surface. The directions in which electrons feel a force concentrated around peaks are illustrated by the yellow arrows. The red line represents the interface between the bulk (above the line) and surface (below the line) electrolyte.

2.3. The Anodic Polarization Curve

Fig. 3 shows the general current density and voltage relationship for an anode in the electropolishing process. The plot of this relationship is known as an anodic polarization curve. Due to the special conditions present at the anode, namely the viscous layer, the polarization curves at the anode and cathode are not identical, so the curve must be specified as "anodic". The current density increases with applied voltage in region I. In region II, however, the current density drops due to the formation of the viscous layer, and plateaus (where it is known as the limiting current density) in region III, the optimal polishing region. The viscous layer then dissolves in region IV,

and current density continues to increase with applied voltage. In this region, significant pitting of the surface occurs. Beyond region IV (not depicted in Fig. 3), the rate of dissolution increases rapidly, and pitting of the surface becomes minimal. Here, polishing can be achieved, but minimizing mass loss on the anode is sacrificed.
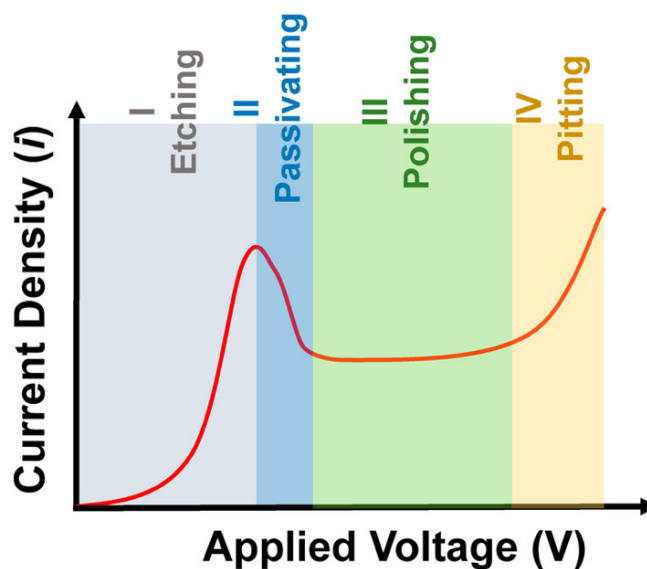

Figure 3: Simplified theoretical Anodic Polarization Curve relating Current Density and Applied Voltage as applied to electropolishing [2]

3. Experimental

3.1. Apparatus Configuration

A system was designed to contain, initiate, and monitor the electrochemical reaction of interest in this experiment—electropolishing. The system consists of two main components: the electrolytic cell (the vessel in which the reaction takes place) and a monitoring and power supply system.

3.1.1. Electrolytic Cell

The electrolytic cell consists of a source of electrical potential difference, an anode and cathode, and an electrolyte through which current can flow. Fig. 4 shows a simplified illustration of the electrolytic cell.

A Teflon block firmly holds two stainless steel counter electrodes and a "claw" like construction holds the sample (coupon) to be electropolished. This unit is then affixed to a vertical metal rod by means of a clamp. The metal rod is conveniently attached to a heated stir plate. The vessel used to hold the electrolyte is a 400 mL beaker containing a stir bar to agitate the solution. This beaker is immersed in a larger beaker filled with water to regulate and mitigate fluctuations in temperature. The aforementioned electrode construction is suspended directly over the 400 mL beaker, so that when an experiment begins it can be lowered into the electrolyte, immersing the electrodes. The electrolyte used during the course of this experiment was composed of 56.7% phosphoric acid, 32% sulphuric acid, and 11.3% water.
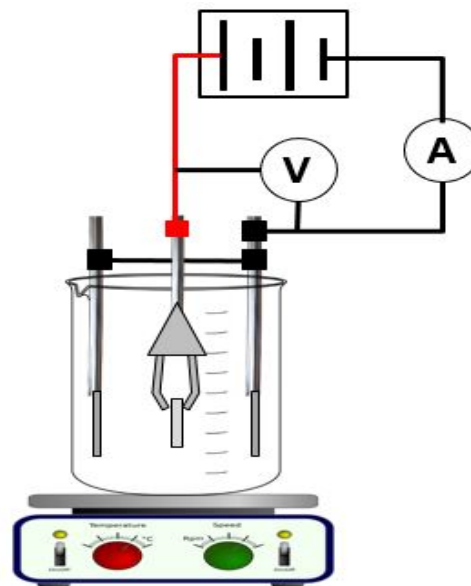

Figure 4: Electrolytic cell illustration. The center anode clip suspends the coupon and is equally spaced between and parallel to the two stainless steel cathode plates. The ammeter and voltmeter are also shown. The water bath immersing the beaker shown and thermocouple have been omitted for clarity.

3.1.2. Monitoring and Power Supply System

The other main component of the apparatus is the data collection and power supply center. This equipment sits on a cart that can be connected to and disconnected from the reaction vessel through a bundle of wires. This ensures that the data acquisition equipment is a safe distance from the electrochemical reaction, and it allows it to be mobile.

The cart consists of a computer on the top shelf, which is equipped with a LabView program to receive data from the experiment and to trigger the power supply. Fig. 5 shows the program display, where the user inputs the experimental parameters and receives real-time data. On the second shelf, there are a power supply, a multimeter, and a National Instruments DAQ (data acquisition) terminal containing three modules: an electromechanical relay, voltage input, and thermocouple input.
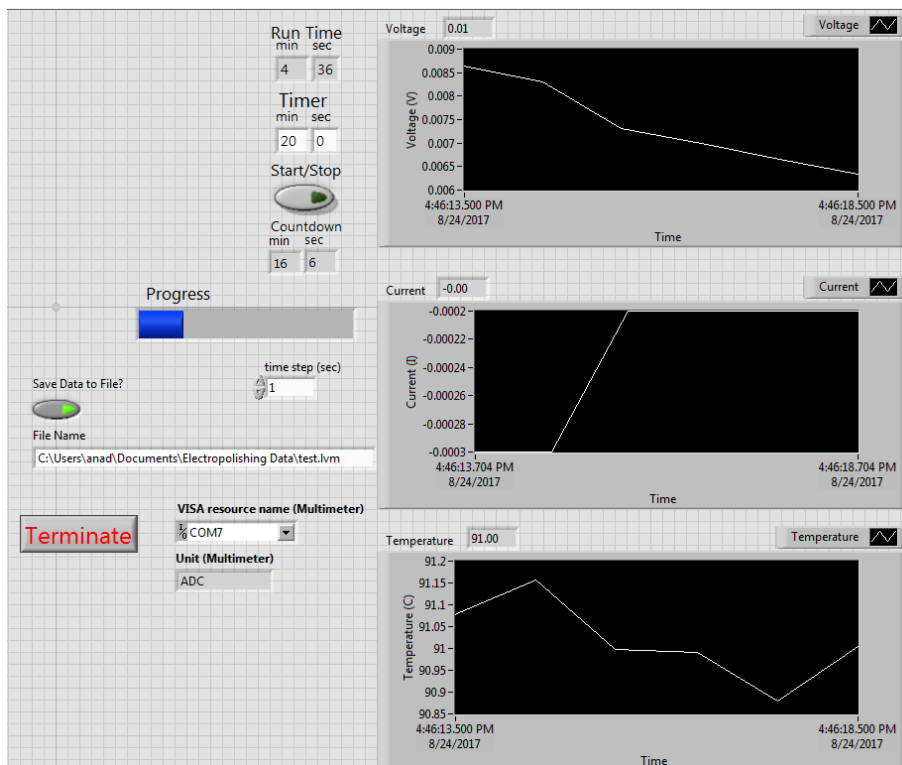
Figure 5: LabView Front Panel. The voltage, current, and temperature readings are updated in real-time. The experimental data is automatically exported and saved to a file.

The multimeter and DAQ terminal are attached to the computer through a USB connection, so that data can be transferred. One end of a pair of wires is attached to the remote control circuit of the power supply, and the other end is attached to the electromechanical relay. When the relay is turned off, an open circuit is created, preventing the power supply from outputting any current, and when the relay is on, a short circuit is created, allowing the power supply to output current.

The power supply, current and voltage monitors, and reaction vessel form a simple circuit shown in Fig. 6. Starting from the power supply output, the negative terminal is attached to the common ground of the multimeter through a wire. Since the multimeter is measuring current, it must be in series with the system. Another wire comes out of the multimeter and terminates at an alligator clip. At the positive terminal of the power supply, a wire extends and also terminates at an alligator clip. The DAQ voltage input module must be connected in parallel with the circuit. Therefore, its positive and negative wires are bundled with the wires coming from the power supply at the alligator clips. The electrolyte solution acts as the main resistor for this simple circuit,

so the alligator clips are attached to the electrodes. It is important to note that for electropolishing, the positive terminal must be attached to the coupon being polished, and the negative terminal to the counter electrode. The opposite is true for electroplating.

The final data analysis unit is the thermocouple module. The positive and negative terminals of the thermocouple DAQ unit are attached to the positive and negative wires of the thermocouple. The thermocouple, power supply, and voltmeter wires lead to the reaction vessel in the fume hood.
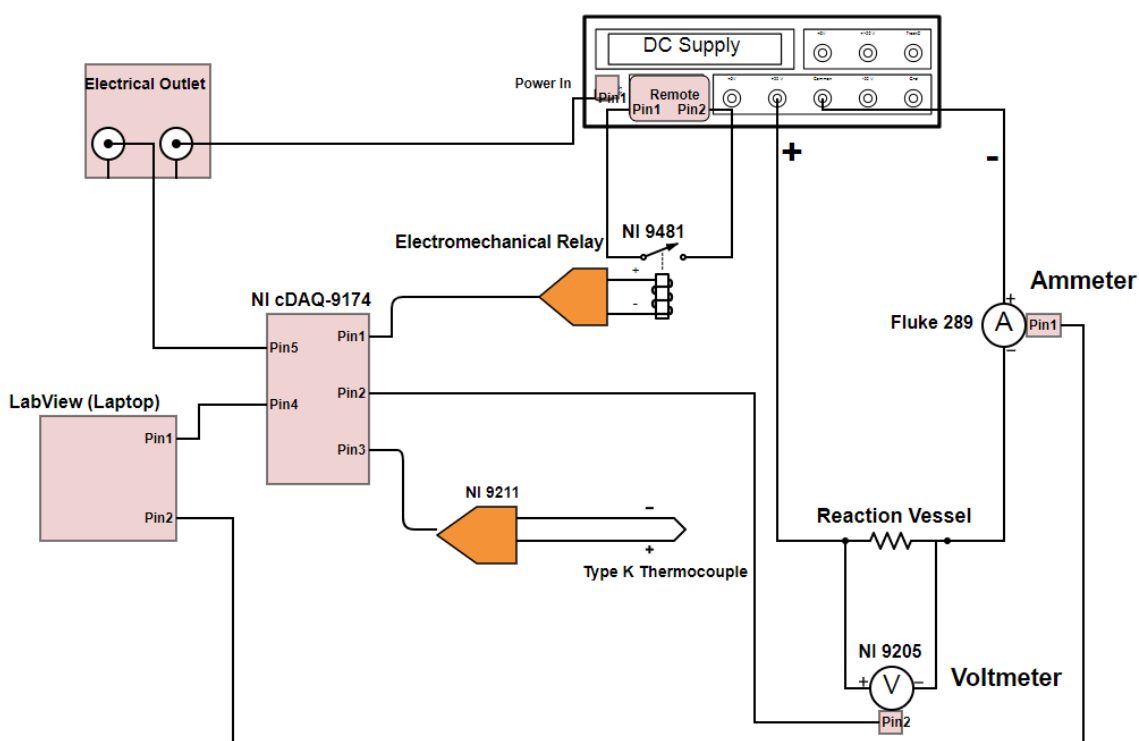

Figure 6: Electrical schematic of the electrolytic cell monitoring and power supply system

3.2. Electropolishing Procedure

3.2.1. Pretreatment

All electropolishing trials begin with the preliminary treatment and analysis of the coupons, which are approximately 16 mm by 20 mm by 3 mm 316 stainless steel samples. The initial step is to mechanically polish the coupons with a ~5 μm diamond paste, and then a 0.3 μm alumina slurry, which is achieved by an outside company. Then, the coupons must be washed in a three-solvent ultrasonic bath with acetone, DI water, and isopropyl alcohol, in order to eliminate any oils and residues left from the mechanical polishing process.

3.2.2. Interferometry

The surfaces of coupons that are to be polished are analyzed thoroughly before and after polishing. The samples are analyzed with an interferometer, a device that takes a detailed three-dimensional surface scan and quantifies its characteristics. Two main surface metrics were chosen: root mean square surface slope (SDQ) and mean height (Sa). The mean height describes a surface's smoothness generally and is commonly seen in literature. The root mean square surface slope gives the mean slope of a sample, which is a more specific description of surface smoothness, as Fig. 7 illustrates. Each coupon was scanned at 40 equally spaced points over both faces and some representative images were saved.
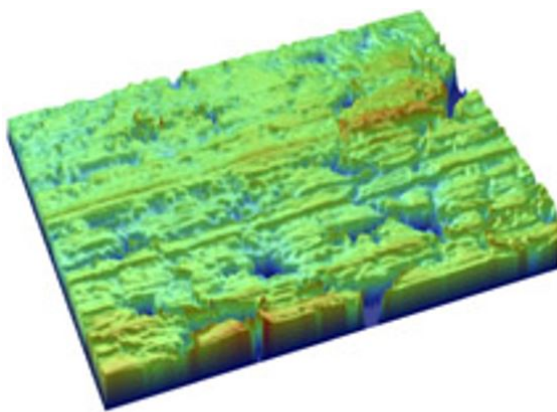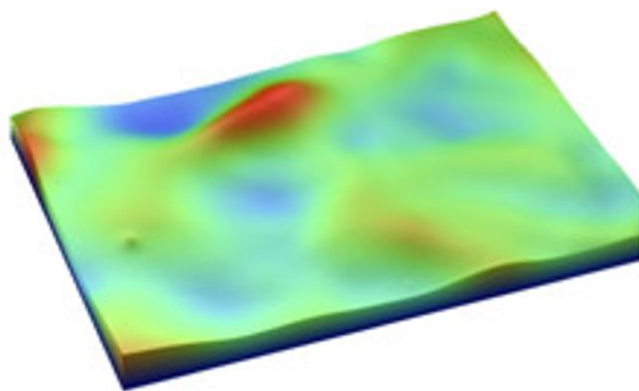
Sa = 80nm, Sdq= 11.0°   **Sa= 75nm, Sdq= 0.2°**

Figure 7: A visibly rough surface on the left and a smooth surface on the right. Note that the Sa values are quite similar, whereas the SDQ values are significantly different.

3.2.3. Voltage Scans and Polarization Curve Production

A variety of voltage scans were conducted at a variety of temperatures to determine how the anodic polarization curves change. The curves were produced by first submersing the electrodes and coupon in the electrolyte and setting the voltage dial on the power supply to 0 V. Then, the program run time was set to an arbitrarily long duration. Once the power supply was switched on, the voltage was gradually increased until reaching approximately 4 V (the point at which little of note would be observed on the polarization curve). The data was exported to an Excel spreadsheet, and the surface area of the coupon was measured. With this information, the current density was calculated and plotted against voltage. Fig. 8 shows an example of a representative polarization curve produced as detailed above. The polarization curves produced were very close in shape to the theoretical model shown in Fig. 3. The optimal polishing voltage can be seen in the plateau region.
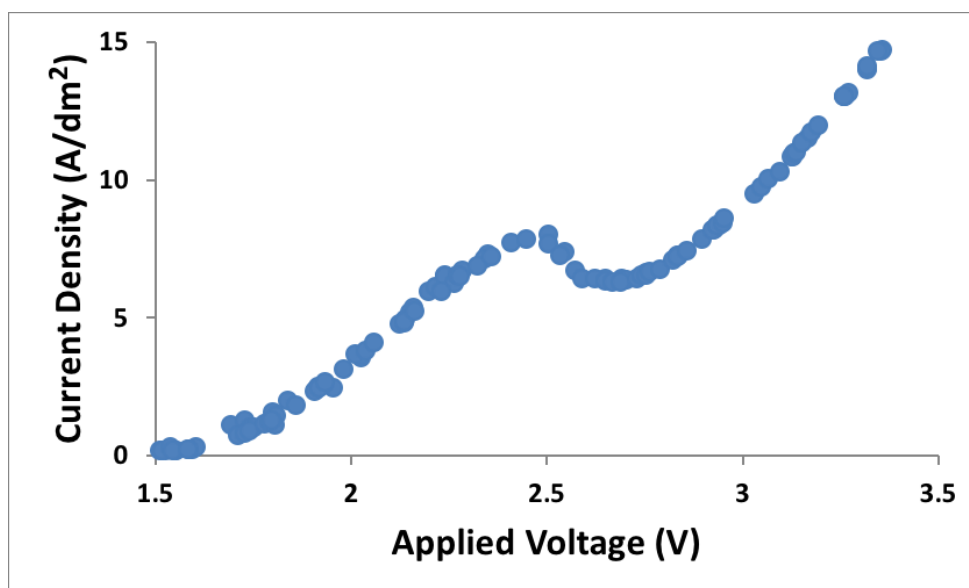

Figure 8: Representative experimentally determined anodic polarization curve with plateau between 2.6 V and 2.8 V. The plateau voltage tended to stay constant over a variety of operating conditions.

3.2.4. Polishing Runs

The mass of the coupon is measured on a scale precise to 10 µg before and after the polishing run. Before the coupon is electropolished, a test coupon is secured to the electrode holding apparatus. Due to the limitations of the power supply, the test coupon must first be submersed in the electrolyte to set the voltage for the trial. The above-mentioned alligator clips are attached to the two electrodes and the thermocouple is secured in the water bath. The multimeter is powered on, and the LabView program is started. The temperature is closely monitored, ensuring that it stays within one degree of the desired temperature. The power supply is then initiated, and the optimal voltage (determined by the location of the plateau on the anodic polarization curve) is set. The power supply is switched off, the desired run time is set in the program, the test coupon is switched out for the coupon to be polished, and the program is initiated, which turns on the power supply. Once the power supply automatically shuts off after the time set in the LabView program has elapsed, the coupon is removed from the corrosive electrolyte bath, and washed with acetone and DI water.

4. Results and Discussion

4.1. Temperature, Agitation Dependence, and the Viscous Layer

The limiting current density (the current density in the plateau region) is highly dependent on the electrolyte bath operating conditions, namely, temperature and solution agitation. The limiting current density i_L is given by [3]

$$i_L = \frac{nFD_0C}{\delta} \exp\left(-\frac{Q_a}{RT}\right) \tag{2}$$

where n is the molar of the total charge of ion involved, D_0 is the exponential pre-factor of the diffusion coefficient of the rate limiting species, C is the saturation concentration of metal ions, δ is the thickness of the viscous layer, Q_a is the activation energy for diffusion, R is the gas constant, and T is the absolute temperature. The viscous layer has been observed as a yellow film visible on the coupon surface during the electropolishing runs. It is expected that its thickness will decrease (decreasing δ) with an increasing bath stir rate, because the agitation will disrupt the layer. The temperature and agitation rate were tested against this theoretical model by generating multiple polarization curves. The limiting current densities of each of these polarization curves were found and plotted as shown in Fig. 9.
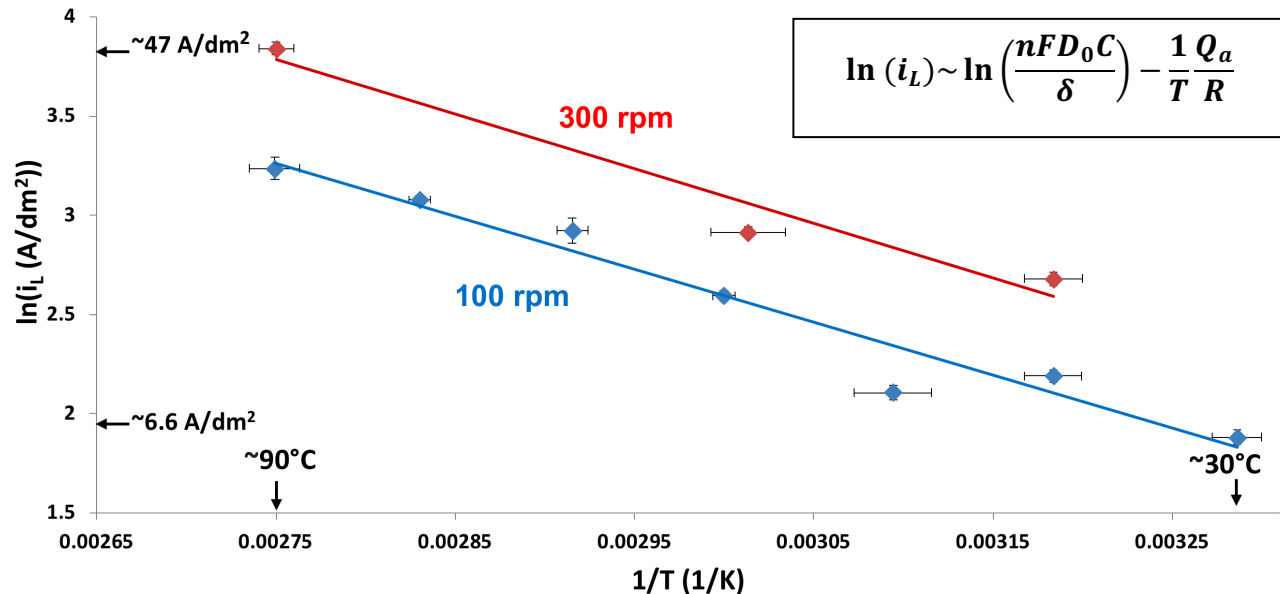
Figure 9: Natural logarithm of the limiting current density plotted against inverse temperature. Temperature and stir rate were varied and the limiting current density changed accordingly. As temperature increased, the limiting current density increased. As the stir rate was increased, the limiting current density also increased.

The linear fit for trials at a stir rate of 100 rpm is approximately parallel to that of trials at a stir rate of 300 rpm, confirming that the activation energy for diffusion is constant. The 300 rpm regression is shifted above the 100 rpm fit, implying that the terms in front of the exponential in equation 2 are greater. The terms n, D_0, and C remain relatively constant for a given electrolyte and anode, leaving only δ, the thickness of the diffusion layer to vary. The data is consistent with equation 2, as the diffusion layer is visibly thinner at a higher stir rate, and the regression model confirms this. Agitation must be kept low enough in order to preserve the viscous layer, cited as being vital for optimal polishing.

4.2. Surface Deformities

Significant surface pitting has been observed on polished coupon samples, caused by the evolution of oxygen at the anode (the coupon) and hydrogen at the cathode, whose reactions are shown in Fig. 1. The plateau voltage is greater than the reversible potential for oxygen evolution, so oxygen bubbles form on the coupon surface. These bubbles disrupt the viscous layer, resulting in a localized attack of the metal surface [4]. This can be mitigated by the removal of those bubbles through the agitation of the solution. Another more significant
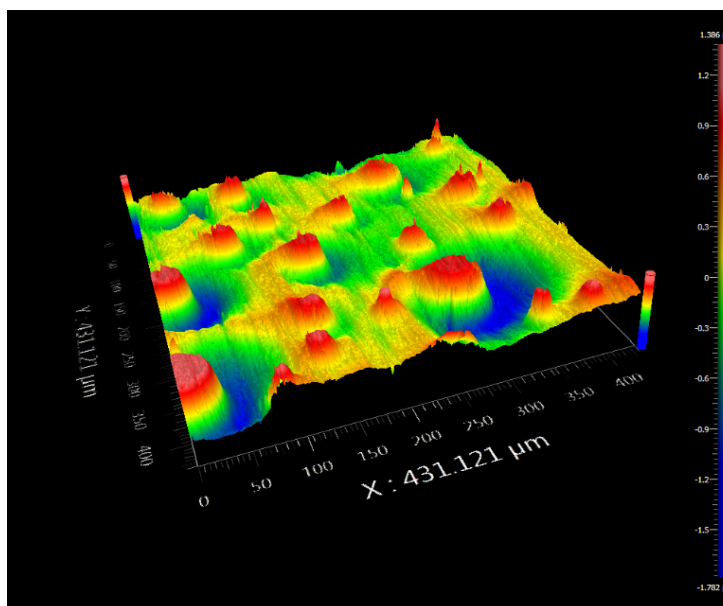

Figure 10: Example of pitting due to hydrogen bubbles. The sample was polished for 30 seconds at a stir rate of 300 rpm. Note the characteristic donut shaped pits. The colors represent surface deformations ranging from -1.78 μm (blue) to +1.39 μm (red).

problem is the evolution of hydrogen at the anode, which occurs at double the rate of oxygen evolution. This is a consequence of the equation for the electrolysis of water, where two moles of hydrogen gas are produced for every mole of oxygen gas. This relatively large amount of hydrogen bubbles disperses into the solution and can be deposited on the anode, due to solution agitation. Donut shaped pits were generated on the surface because of the occlusion of the surface below and increased attack in the surrounding regions [4]. Fig. 10 is an example of this type of pitting observed on multiple coupons. These pits, as opposed to those resulting from oxygen bubbling, can be prevented by reducing solution agitation. It follows that the stirring rate must be chosen very carefully in order to preserve the viscous layer, to prevent oxygen bubbling, and to prevent hydrogen bubbling.

4.3. Polishing above the Plateau

      Although optimal polishing is cited to occur in the plateau region, noteworthy results can be obtained at higher voltages. Fig. 11 shows the effects of changing voltage on coupon surface finish.
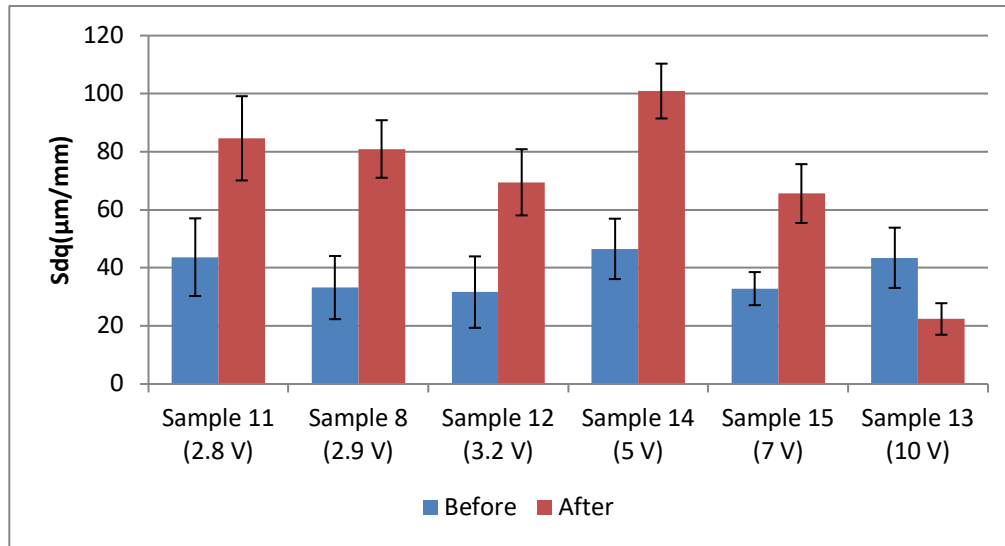

Figure 11: Root mean square surface slope on the Y axis and Voltage on the X axis before and after polishing. All samples polished at 21 C for 10 minutes. Note that the 10 V trial is the only one that saw a decrease in SDQ, and therefore a reduction in surface roughness. Here, SDQ is expressed as the tangent of the angle, as done commonly. An SDQ of 100 µm/mm corresponds to an angle of 5.71°.

      At all voltages between 2.8 V and 10 V (between the end of the optimal polishing region through region IV [see Fig. 3]), the surface finish worsens after polishing. The trial run at 10 V, however, results in a significant decrease in SDQ and a visibly more reflective surface. At this voltage, the viscous layer cannot form, so a high metal ion concentration gradient is not present at the surface of the coupon. Polishing beyond region IV (the 10 V trial is hypothesized to be in this range), as discussed in relation to Fig. 3, rapidly dissolves the metal surface. Dissolution occurs at approximately the same rate over the surface, which results in significant erosion. The results of polishing far beyond the plateau voltage can be seen in Fig. 12.
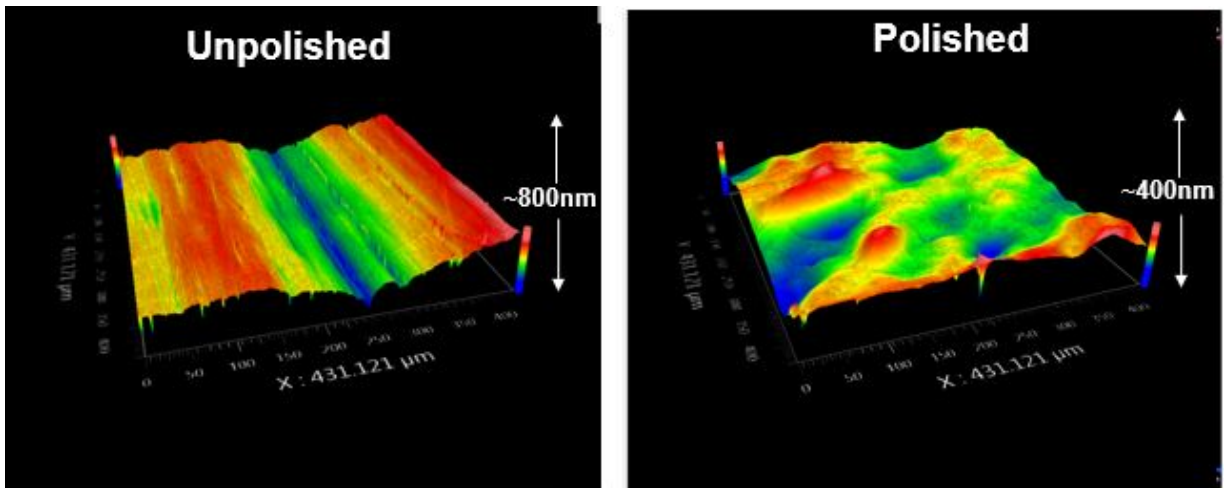
Figure 12: Unpolished coupon on the left. Sample polished for 30 minutes at 12V on the right. SDQ decreased 63.2%. Mass decreased 16%, and thickness decreased 179.3µm. The optimal thickness loss for applications requiring tight-fitting machined components is ~1µm. The white arrows indicate the approximate range of surface deformities from peak to valley.

Polishing above the plateau for prolonged periods of time dramatically reduces the surface roughness. This however, comes with a drawback—a substantial amount of metal is removed from the coupon. The decrease in mass observed in the trial in Fig. 12 is unacceptable for applications requiring tight-fitting machined components.

4.4. The Loss of Material in Electropolishing

The loss of mass from a coupon during electropolishing is proportional to the amount of charge applied, the product of current and time. This is quantified by equation 1, Faraday's Law of Electrolysis. Fig. 13 shows a plot of the theoretical mass loss and actual mass loss as a function of applied charge.
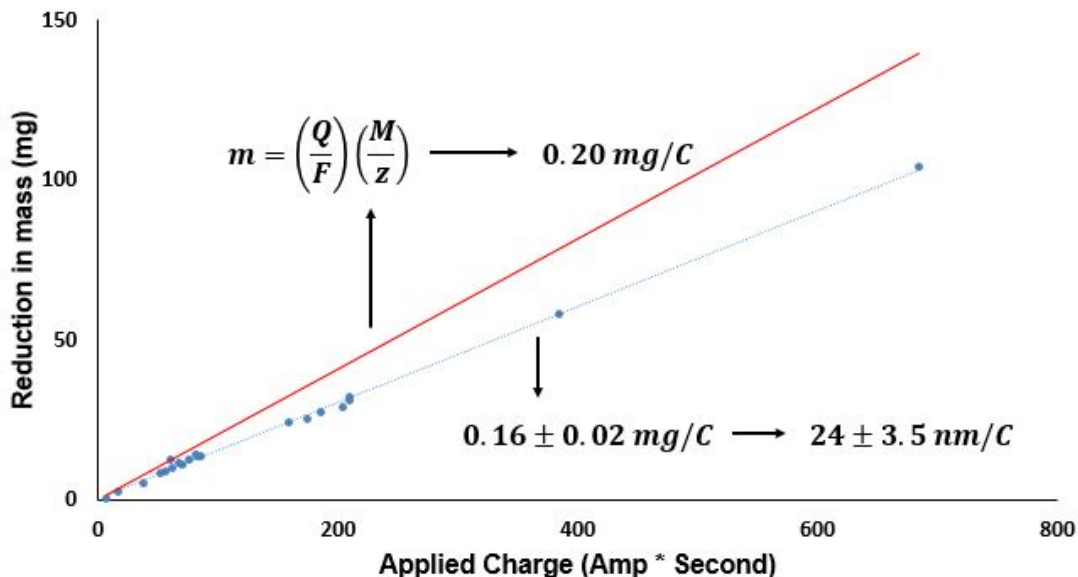
Figure 13: Mass reduction plotted against charge applied predicted by Faraday's Law of Electrolysis (red) and experimentally determined (blue). Appropriate values of M, molar mass of the metal, and z, valency of metal ions, were substituted into equation 1. The mass lost is 76% of that predicted by Faraday's Law. The thickness loss equivalent of 24±3.5 nm/C was calculated by considering the density of the stainless steel and surface area of the coupons.

The actual reduction in mass is consistently proportional to the amount of charge applied. This provides a powerful predicting tool for applications in this experimental setup. A certain amount of material can be removed with relative precision, by supplying a known current (investigated in Fig. 9) for a certain amount of time.

5. Conclusion and Further Steps

The mechanism of electropolishing was investigated and theory was applied in order to probe the effect of operating conditions on surface finish. Electropolishing is a problem in optimization, so a careful balance must be found between operating parameters. Tradeoffs have to be made between surface roughness and the thickness removed, as they are inversely related. If too much charge is applied to the sample, its roughness will decrease significantly, but more material will be lost. If too little charge is applied, the roughness will not change significantly, but less material will be lost. Additionally, the stirring rate and temperature need to be carefully controlled in order to preserve the all-important viscous layer and, at the same time, prevent pitting.

The optimal conditions are a lower total charge, careful stirring, and a higher electrolyte temperature to increase the limiting current density. Progress has been made toward optimizing these factors, and the electropolishing system is better understood. The next steps include moving toward a pulsed power system, where DC current is supplied intermittently. This would limit the formation of bubbles and lead to a less pitted surface. An inventory of samples should also be assembled to be chemically analyzed, as electropolishing changes not only the physical properties of a surface, but also the chemical properties.

6. Acknowledgements

7. References

[1] W. T. Shmayda, M. Sharpe, C. Fagan, and W. U. Shroder, Laboratory for Laser Energetics, unpublished.

[2] D. Landolt, "Fundamental Aspects of Electropolishing," *Electrochimica Acta*, Vol. 32, No. 1, pp. 1-11, 1987.

[3] G. Yang, B. Wang, K. Tawfiq, H. Wei, S. Zhou & G. Chen (2017) Electropolishing of Surfaces: Theory and Applications, Surface Engineering, 33:2, 149-166, DOI: 10.1080/02670844.2016.1198452

[4] A. Chandra, 2012, 'On the Mechanism of Niobium Electropolishing', Graduate Program in Materials Science and Engineering, The Ohio State University.